Author Manuscript

Author Manuscript

Author Manuscript

Author Manuscript

HHS Public Access

Author manuscript

Dev Biol. Author manuscript; available in PMC 2022 March 01.

Published in final edited form as:

Dev Biol. 2021 March ; 471: 97–105. doi:10.1016/j.ydbio.2020.12.011.

Physiological electric fields induce directional migration of mammalian cranial neural crest cells

Abijeet Singh Mehta[1,2,#], **Pin Ha**[3,#], **Kan Zhu**[1,2,#], **ShiYu Li**[1,2], **Kang Ting**[3], **Chia Soo**[4], **Xinli Zhang**[3,¶], **Min Zhao**[1,2,¶]

[1]Department of Ophthalmology & Vision Science, Institute for Regenerative Cures, Center for Neuroscience, University of California at Davis, School of Medicine, Suite 1630, Room 1617, 2921 Stockton Blvd., Sacramento, CA, 95817, USA.

[2]Department of Dermatology, University of California, Davis, CA, USA.

[3]Section of Orthodontics, Division of Growth and Development, School of Dentistry, University of California, Los Angeles, CA, USA.

[4]Division of Plastic and Reconstructive Surgery and Department of Orthopaedic Surgery and the Orthopaedic Hospital Research Center, University of California, Los Angeles, CA 90095, USA

Abstract

During neurulation, cranial neural crest cells (CNCCs) migrate long distances from the neural tube to their terminal site of differentiation. The pathway traveled by the CNCCs defines the blueprint for craniofacial construction, abnormalities of which contribute to three-quarters of human birth defects. Biophysical cues like naturally occurring electric fields (EFs) have been proposed to be one of the guiding mechanisms for CNCC migration from the neural tube to identified position in the branchial arches. Such endogenous EFs can be mimicked by applied EFs of physiological strength that has been reported to guide the migration of amphibian and avian neural crest cells (NCCs), namely galvanotaxis or electrotaxis. However, the behavior of mammalian NCCs in external EFs has not been reported. We show here that mammalian CNCCs migrate towards the anode in direct current (dc) EFs. Reversal of the field polarity reverses the directedness. The response threshold was below 30mV/mm and the migration directedness and displacement speed increased with increase in field strength. Both CNCC line (O9–1) and primary mouse CNCCs show similar galvanotaxis behavior. Our results demonstrate for the first time that the mammalian CNCCs respond to physiological EFs by robust directional migration towards the anode in a voltage-dependent manner.

[¶]corresponding authors: MZ: minzhao@ucdavis.edu, XZ: xzhang@dentistry.ucla.edu.
[#]contributed equally

Publisher's Disclaimer: This is a PDF file of an unedited manuscript that has been accepted for publication. As a service to our customers we are providing this early version of the manuscript. The manuscript will undergo copyediting, typesetting, and review of the resulting proof before it is published in its final form. Please note that during the production process errors may be discovered which could affect the content, and all legal disclaimers that apply to the journal pertain.

Competing interests
None

Author Manuscript Author Manuscript Author Manuscript Author Manuscript

Keywords

Galvanotaxis; Electrotaxis; Cranial neural Crest Cells; O9-1; Electric fields; Directional cell migrations; Mouse

INTRODUCTION

Neural crest cells (NCCs), a “fourth germ layer”, is innovation that developed in vertebrates as they evolved from protochordates (Hall, 2000; Hu et al., 2014). It facilitated the generation of novel vertebrate head structures that contributed to chordate diversity and adaptation to most niches of the planet. Originally identified by William His in 1868, NCCs originate from the dorsal half of the developing neural tube (Ruhrberg and Schwarz, 2010). During neurulation, dorsal neuroepithelial cells undergo epithelial-to-mesenchymal transition (EMT), followed by a rostrocaudal emigrational wave of NCCs to the terminal site of differentiation (Baker and Bronner-Fraser, 1997; Litsiou et al., 2005). Based on their axial position of origin, and differentiating lineage, NCCs can be categorized as cranial, sacral, vagal, or trunk (Barlow et al., 2012; Hall, 2000; Walker and Trainor, 2006). Cranial neural crest cells (CNCCs) can be considered as multipotent progenitors that can differentiate into most of the cartilage and bone of the skull, face, and pharyngeal skeleton (Crane and Trainor, 2006). They can migrate long distances, from the neural tube to the branchial arches, with the aim of sculpting a scaffold for vertebrate craniofacial development (Trainor, 2010; Trainor et al., 2002). Three-quarters of human birth defects involve craniofacial abnormalities. Annual treatment cost for children born with cleft lip and/ or cleft palate alone is US$697 million (Cordero et al., 2011; Trainor, 2010). This highlights the importance of studying how CNCCs establish stereotypical directional migratory behavior and acquire positional identity to architect the destined structure (Craniofacial) (Mehta and Singh, 2019; Minoux and Rijli, 2010).

CNCCs detect various micro environmental cues that guide their long distance migration (Epperlein et al., 2007; Gilbert et al., 2007; Golding et al., 2000; Gov, 2007; Kulesa and Fraser, 1998; Reyes et al., 2010; Wynn et al., 2013). Significant progress has been made in underpinning the molecular mechanisms and gene regulatory networks that are crucial for targeted CNCC migration (Litsiou et al., 2005; Minoux and Rijli, 2010). In recent years, considerable progress has also been made to identify environmental cues (chemoattractant and mechanical signals) that are involved in long distance migration of CNCCs (Abzhanov et al., 2006; Bajanca et al., 2019; Barriga et al., 2018; Marcucio et al., 2005; Shellard and Mayor, 2019; Szabó et al., 2019; Walheim et al., 2012).

Endogenous EFs are present during neurulation (Metcalf et al., 1994; Shi and Borgens, 1995). During amphibian embryogenesis electric current is driven out of the lateral margins of the neural tube, and out of the blastopore, and returns inward at the neural grove and at the lateral skin, creating an EF gradient of 27 ± 4 mV/mm along the rostral-caudal axis, which changes temporally during neurulation (Hotary and Robinson, 1994; Metcalf et al., 1994; Shi and Borgens, 1995). Manipulating these electric fields (EFs) caused

Author Manuscript Author Manuscript Author Manuscript Author Manuscript

neurocristopathies, e.g. retarded eye development and reduced head formation (Hotary and Robinson, 1994), suggesting contributing role of the EFs.

Applied EFs of physiological strength can guide direction cell migration, suggesting involvement of EFs in directed cell migration (Chang and Minc, 2014; Levin et al., 2017; Levin et al., 2019; Mathews and Levin, 2018). Different putative sensors have been suggested that can determine cell directedness (Allen et al., 2013; Forrester et al., 2007; Kennard and Theriot, 2020; Zhao et al., 2020). In culture, avian and amphibian NCCs respond to applied EFs by directional migration (galvanotaxis / electrotaxis) towards the cathode (Cooper and Keller, 1984; Gruler and Nuccitelli, 1991; Nuccitelli and Smart, 1989). It is however not known whether mammalian NCCs respond to EFs, and what is their preferred directedness. We report here that a well-characterized cranial NCC line, 'O9–1' showed robust directional migration toward the anode in applied EFs, and primary cultures of NCCs of the same cranial lineage had the same anodal galvanotaxis.

MATERIALS AND METHODS

Cell Culture

O9–1 mouse CNCC line is an extended culture of primary CNCCs isolated from E8.5 mouse embryo, which express NCC markers, and can differentiate into osteoblasts, chondrocytes, smooth muscle cells, and glial cells (Ishii et al., 2012). The O9–1 cell line (Sigma Millipore, Cat# SCC049) was cultured in cell culture flasks pre-coated with 1:50 diluted Matrigel™ (Fisher, Cat# CB-40234) at room temperature for 1 hour; then cells were grown in complete ES cell medium with 15% FBS and LIF (Sigma Millipore, Cat# ES-101-B) + 25 ng/ml recombinant human bFGF (Sigma Millipore, Cat# GF003) at 37 °C, 5% CO_2. Primary mouse CNCCs were isolated from the frontal and nasal bones of the cranial vault of neonatal wildtype C57BL/6J mouse, following the established protocol (Chen et al., 2019; Wong and Cohn, 1975; Zhang et al., 2002). They were cultured in growth medium containing high glucose DMEM + 10% heat-inactivated fetal bovine serum (FBS) + 100 U/ml penicillin/streptomycin (P/S) at 37 °C, 5% CO_2. Passage 3–5 of primary cells were used. The animals use was approved by the UCLA IACUC committee.

Real-time quantitative polymerase chain reaction (RT-qPCR)

Real-time PCR was performed using the QuantStudio™ 3 real-time PCR System instrument (Applied Biosystems, Foster City, CA, USA) as described previously (Ishii et al., 2012; James et al., 2015; Mehta et al., 2019; Mehta and Singh, 2017). A set of representative genes of NCCs were selected to define the cells in this study (Ishii et al., 2012; Szabo and Mayor, 2018; Trainor, 2005) (Table 1). All data are representative of three experimental set of cells with PCR triplicates and are presented as the fold change.

Alkaline phosphatase (ALP) and mineralization assays

Osteogenic differentiation of CNCCs is assayed using the leukocytes ALP staining Kit (Sigma-Aldrich, Cat# 86R-1KT) and Alizarin Red (AR) staining with 2% Alizarin Red stains (Lifeline, Cat# CM-0058) (Chen et al., 2019). On Day-7 of initiation of differentiation, the cells were fixed in 4% paraformaldehyde and incubated with a mixture of

Author Manuscript Author Manuscript Author Manuscript Author Manuscript

Naphthol AS-BI alkaline solution and FRV-alkaline solution. Areas that stained pink or light purple were designated as positive. For AR staining, on Day-21, cells were fixed in 4% paraformaldehyde and incubated with 2% Alizarin Red stains. Calcification nodules were stained bright red after thorough wash with water.

Galvanotaxis assay and time lapse imaging

Galvanotaxis experiments were done as described previously (Cooper and Keller, 1984; Song et al., 2007). CNCCs were loaded into the electrotactic chamber (pre-coated with 1:50 diluted Matrigel™) with a density of ~100 cells per square millimeter. The cells were incubated for 4 hours at 37°C with air containing 5% CO_2 to allow attachment. Agar/saline (100% Steinberg's solution gelled with 1% agar) bridges were placed into the chamber channels and connected to wells containing 100% Steinberg's solution and silver-silver chloride electrodes. Time-lapse images of 5-min intervals of cells were acquired using an inverted microscope (Carl Zeiss, Oberkochen, Germany).

ImageJ (National Institutes of Health) software was used to analyze cell migration as described (Song et al., 2007). 'Directedness' is the quantitative measurement of how directionally cells migrated in response to an EF. The directedness was assessed as cosine θ, in which θ was the angle between EF direction and a straight line that connects the start and end positions of a cell. A cell moving directly to the cathode or the anode would have a directedness value of 1 or −1, respectively. Migration distance (in μm) is calculated as (1) accumulated distance, which is the full trajectory distance traveled by the cell, and (2) Euclidean distance, which is the straight-line distance between the starting and final positions of a cell. Displacement speed (in μm/min) is the Euclidean distance over time.

Statistics

Statistical analysis was performed using unpaired, two tailed student *t*-test. Data are expressed as mean ± SEM. *P*-value less that 0.05 was considered statistically significant.

RESULTS

Mammalian CNCCs show anodal galvanotaxis

We first determined the migratory response of mammalian CNCCs O9–1 line to applied EFs. In control condition without EFs, cells migrated actively in random direction (Fig. 1, A,B and Movie 1). When a direct current (dc) EF was applied, the cells showed robust directional migration towards the anode (Fig. 1, C,D and Movie 2).

This noteworthy impact on the migration directedness of O9–1 cells, imposed by a dcEF, is further illustrated by reversing the field polarity. We reversed the EF polarity after CNCCs have been exposed to an EF and migrated for 2h in one direction, then reversed the field direction 180°. In the first 2h, as expected cells migrated towards the anode (left) (Fig 1. E,F and Movie 3). Within 5–10 minutes following the polarity reversal, cells started migrating towards the new anode (right) (Fig1. E,G and Movie 3). The migration trajectories of the individual cells show the directional change upon reversal of the field polarity (Fig 1. F,G). O9–1 cells in culture thus showed anodal galvanotaxis.

Author Manuscript Author Manuscript Author Manuscript Author Manuscript

Voltage dependent responses of mammalian CNCCs

To determine the threshold voltage for galvanotaxis of O9–1 cells, we applied EFs of different strength. We found that at the low field strength of 15 mV/mm, CNCCs did not show statistically significant change in migration direction (Fig 2. A,G and Movie 4). However, in a field with strengths of 30 mV/mm and greater, CNCCs show statistically significant directional migration towards the anode (Fig 2. B–G and Movie 4), suggesting that the threshold for O9–1 cell galvanotaxis is between 15mV/mm – 30mV/mm (Fig 2. B,G).

Displacement speed of O9–1 cells show progression with the increase in EF strengths (Fig 2. H). The displacement speed in the absence of EF is 0.45 ± 0.04 (μm/mm), which significantly increased to 0.829 ± 0.08 in an EF of 30 mV/mm and continues to increase with the increase in field strength. The threshold for increased displacement speed is likely between 15–30mV/mm.

Galvanotaxis of primary cultures of CNCCs

Next, to rule out any cell line specific response, we used primary cultures of CNCCs to test galvanotaxis of the same cranial lineage. The primary cells were from the frontal and nasal bones of neonatal wildtype (C57BL/6J) mouse cranial vault (Fig 3. A). This region in mouse is derived only from CNCCs (Chen et al., 2020; Jiang et al., 2002). The primary cells were validated for their CNCC properties by performing RT-qPCR of representative markers (*Snail1, Twist1, Nestin*, *CD44* and *Sca-1*) (Ishii et al., 2012; Szabo and Mayor, 2018; Trainor, 2005) (Fig 3. B). Expression of those markers were confirmed in the O9–1 cells as well, which were used to normalize expression levels in the primary cells. Also, differentiation potentials of both O9–1 and primary CNCCs were tested for osteogenesis (Fig 3. C). Potency of osteogenesis distinguishes CNCCs from other NCC populations (Le Douarin and Kalcheim, 1999; Noden, 1988; Santagati and Rijli, 2003; Szabo and Mayor, 2018). We placed cells in osteogenic conditions and performed ALP staining and AR staining at different time points (Day-7 and Day-21 following differentiation induction). Both types of cells achieved positive ALP activity, and mineralization stained by AR (Fig 3. C).

We recorded voltage dependent response of primary CNCCs. Similar to cell lines (O9–1), directed migration of primary CNCCs also improved with increasing field strength (Fig 3. D–I and Movie 5,6). Effect on migration directedness became significant at 100mV/mm, and further at 200mV/mm. The effect on displacement speed however, started to show significance even at much lower field strength of 15mV/mm, which was further increased at 100–200mV/mm (4–5 times faster than that of no EF control) (Fig 3. I).

Culture density of CNCCs did not affect galvanotaxis

We finally asked whether galvanotaxis of CNCCs is affected by the cell culture density. Cell-cell contact has been shown to be important in chemotaxis of NCCs (Kasemeier-Kulesa et al., 2006; Kasemeier-Kulesa et al., 2005; Krull et al., 1995; Theveneau et al., 2010). The CNCCs migrate in three streams from the hindbrain, and cells within these streams often form chainlike arrays, in which they maintain contact and migrate collectively. CNCCs

Author Manuscript Author Manuscript Author Manuscript Author Manuscript

migrating together in chain have higher directionality then cells migrating individually (Kulesa and Fraser, 1998; Teddy and Kulesa, 2004). Therefore, we studied galvanotaxis in high density culture (approx. 620 cell/mm^2), in which cells maintained multiple cell-cell contact. (Fig. 4, and Movie 7). Galvanotaxis of the cells in high cell density cultures turned out to be very similar to that of low-density cultures (approx. 150 cell/mm^2) under the same strength of EF (15, 30, 50, 75, 100, and 200 mV/mm) (Fig 4. A–F, H and Movie 7 vs. Fig 2. A–F, Fig 4. G, and Movie 4). The directedness of high density CNCCs is slightly higher (Fig 4. I), and displacement speed is slightly lower (Fig 4. J) for every tested voltage strength but without statistical significance.

DISCUSSION

Our results demonstrate that (1) mammalian CNCCs migrate towards the anode in applied dcEFs of physiological strength; (2) Directedness, and displacement speed are voltage-dependent with threshold likely to be between 15–30mV/mm, very similar to the fields measured *in vivo* (27 ± 4 mV/mm) (Hotary and Robinson, 1994; Metcalf et al., 1994).

NCCs, arising over the vertebrate axis, start to emigrate from the midbrain region in chick at approximately five to six somite stage (embryonic day (E) 1.5) (Tosney, 1982), xenopus at stage 12 (Sadaghiani and Thiébaud, 1987), zebrafish at 13–14 hr postfertilization (Schilling and Kimmel, 1994), and in mouse at five somite stage (E8.25) (Nichols, 1986). The migration is critical for development and the underlying mechanisms have been investigated, mostly for chemotaxis, and more recently for durotaxis (Barriga et al., 2018; Dyson et al., 2018; Shellard and Mayor, 2019; Shellard et al., 2018; Szabo and Mayor, 2018).

Naturally occurring EFs in embryos and galvanotaxis of NCCs

Endogenous EFs occur naturally in embryos. The activity of various ion pumps and transporters generate charge difference across the epithelium that is manifested as transepithelial potential (TEP) (Kennard and Theriot, 2020; Shi and Borgens, 1995). The TEP across the embryonic ectoderm is the driving force capable of producing ionic-current flow through, and out, of the embryos at the region of low electric resistance. This current flow in turn sets up endogenous EFs within the embryos (Metcalf and Borgens, 1994; Metcalf et al., 1994). TEPs have been recorded during blastula, gastrula, and neurula stages in amphibian, in primitive streak, during later stages development in the chick, and have also been suggested in mouse blastomeres (Jaffe and Stern, 1979; McCaig and Robinson, 1982; Metcalf et al., 1994; Nuccitelli, 1992; Nuccitelli and Wiley, 1985; Regen and Steinhardt, 1986). Modification of these fields during neurulation can cause developmental abnormalities (Nuccitelli, 2003). It was suggested that EFs in the range of 20–200 mV/mm exist along the migration pathways of NCCs.

Avian and amphibian NCCs in culture showed directional migration, even in an EF as low as 7mV/mm (Nuccitelli et al., 1993). Our results add experimental evidence that mammalian cranial NCCs also have robust galvanotaxis response. The threshold of EFs to increase displacement speed and to induce directional migration appears to lie between 15–30 mV/mm (Figs. 2, 3, 4). These threshold values fall into the voltage gradients detected in avian and amphibian embryos (Jaffe and Stern, 1979; McCaig and Robinson, 1982; Metcalf

Author Manuscript Author Manuscript Author Manuscript Author Manuscript

et al., 1994; Nuccitelli, 1992; Nuccitelli and Wiley, 1985; Regen and Steinhardt, 1986). Another interesting point is that the directedness values of galvanotaxis in threshold fields seem fall in the range of average migration directionality of NCC in vivo from (0.19 ± 0.1 to 0.3 ± 0.1) (Kulesa et al., 2004; Kulesa and Fraser, 1998) (Fig. 2G and Fig. 3H).

Anode vs. cathode galvanotaxis of NCCs

The avian and amphibian NCCs migrate toward the cathode (Cooper and Keller, 1984; Gruler and Nuccitelli, 1991). Mouse CNCCs, however, showed anodal galvanotaxis, opposite to previous reported cathodal migration of avian and amphibian NCCs. In the absence of EFs, CNCCs are flatter, have multipolar protrusions with no preferential direction of cell protrusion and migration (movie 1). CNCCs in EFs assume a morphology with long bipolar filipodia perpendicular to the field line, and smaller active protrusions projected in the direction of migration (Movie 2). Cell membrane protrusions in the direction of migration is consistent with that reported *in vitro* as well as *in vivo* (Dang et al., 2013; Kennard and Theriot, 2020; Pollard and Cooper, 2009).

Why is there such a contrasting difference in galvanotaxis direction? We speculate that the difference may be due to lineage difference (cranial vs trunk population), developmental stage, and/or due to different species from which cells have been isolated. CNCCs are a special group of NCCs that have osteogenesis potential (Le Douarin and Kalcheim, 1999; Noden, 1988; Santagati and Rijli, 2003; Szabo and Mayor, 2018). Osteogenesis property were confirmed in both the O9–1 and primary cells (Fig. 3 C). CNCCs also have very distinct gene expression profiles, different from the trunk NCCs (Hu et al., 2014; Rothstein et al., 2018). It was suggested that axial-specific genetic circuits operate in each subpopulation and underlie their unique features. Such phylogenic difference may impact vertebrate evolution (Clay and Halloran, 2010; Kuo and Erickson, 2011; Rothstein et al., 2018). NCCs used in previous studies were more likely to be the trunk subpopulations from earlier stage of development. Species difference might be another possible reason, because mammalian NCCs have some unique features (Barriga et al., 2015; Simões-Costa and Bronner, 2015). Indeed, species difference in NCC migration is recently been elegantly demonstrated with ray-finned fishes (Stundl et al., 2020).

In conclusion, externally applied EFs with a threshold voltage between 15–30mV/mm direct mammalian CNCCs to migrate towards the anode with increased displacement speed. This threshold voltage is of the size reported in embryos. Galvanotaxis alongside well-elucidated chemotaxis and durotaxis, is likely to regulate NCC migration. Further investigation is warranted to determine galvanotaxis in guiding migration of NCCs in development, especially the craniofacial development.

Supplementary Material

Refer to Web version on PubMed Central for supplementary material.

Acknowledgment

We thank Dr. Brian Reid for proofreading and editing the manuscript.

Author Manuscript Author Manuscript Author Manuscript Author Manuscript

Funding

This work is supported by the AFOSR-MURI grant FA9550-16-1-0052, and NIH 1R01EY019101. This study was also supported by the NIH (grants R01AR066782, R01AR068835, R01DE029353), UCLA/NIH CTSI (grant UL1TR000124). Work in Zhao Laboratory is also supported by NEI Core Grant (P-30 EY012576, PI. Jack Werner / Marie Burns) and a DARPA Award (HR001119S0027) (Lead PI Dr. Marco Rolandi, UC Santa Cruz). We are also grateful to the following support: Louis and Karen Burns family donation, Unrestricted Grant from Research to Prevent Blindness, Inc.

References

Abzhanov A, Kuo WP, Hartmann C, Grant BR, Grant PR, Tabin CJ, 2006 The calmodulin pathway and evolution of elongated beak morphology in Darwin's finches. Nature 442, 563–567. [PubMed: 16885984]

Allen Greg M., Mogilner A, Theriot Julie A., 2013 Electrophoresis of Cellular Membrane Components Creates the Directional Cue Guiding Keratocyte Galvanotaxis. Current Biology 23, 560–568. [PubMed: 23541731]

Bajanca F, Gouignard N, Colle C, Parsons M, Mayor R, Theveneau E, 2019 In vivo topology converts competition for cell-matrix adhesion into directional migration. Nature communications 10, 1518–1518.

Baker CVH, Bronner-Fraser M, 1997 The origins of the neural crest. Part I: embryonic induction. Mech Dev 69, 3–11. [PubMed: 9486527]

Barlow AJ, Dixon J, Dixon MJ, Trainor PA, 2012 Balancing neural crest cell intrinsic processes with those of the microenvironment in Tcof1 haploinsufficient mice enables complete enteric nervous system formation. Hum Mol Genet 21, 1782–1793. [PubMed: 22228097]

Barriga EH, Franze K, Charras G, Mayor R, 2018 Tissue stiffening coordinates morphogenesis by triggering collective cell migration in vivo. Nature 554, 523–527. [PubMed: 29443958]

Barriga EH, Trainor PA, Bronner M, Mayor R, 2015 Animal models for studying neural crest development: is the mouse different? Development (Cambridge, England) 142, 1555–1560.

Chang F, Minc N, 2014 Electrochemical control of cell and tissue polarity. Annu Rev Cell Dev Biol 30, 317–336. [PubMed: 25062359]

Chen X, Wang H, Yu M, Kim JK, Qi H, Ha P, Jiang W, Chen E, Luo X, Needle RB, Baik L, Yang C, Shi J, Kwak JH, Ting K, Zhang X, Soo C, 2019 Cumulative inactivation of Nell-1 in Wnt1 expressing cell lineages results in craniofacial skeletal hypoplasia and postnatal hydrocephalus. Cell Death Differ.

Chen X, Wang H, Yu M, Kim JK, Qi H, Ha P, Jiang W, Chen E, Luo X, Needle RB, Baik L, Yang C, Shi J, Kwak JH, Ting K, Zhang X, Soo C, 2020 Cumulative inactivation of Nell-1 in Wnt1 expressing cell lineages results in craniofacial skeletal hypoplasia and postnatal hydrocephalus. Cell Death & Differentiation 27, 1415–1430. [PubMed: 31582804]

Clay MR, Halloran MC, 2010 Control of neural crest cell behavior and migration: Insights from live imaging. Cell Adh Migr 4, 586–594. [PubMed: 20671421]

Cooper MS, Keller RE, 1984 Perpendicular orientation and directional migration of amphibian neural crest cells in dc electrical fields. Proc Natl Acad Sci U S A 81, 160–164. [PubMed: 6582473]

Cordero DR, Brugmann S, Chu Y, Bajpai R, Jame M, Helms JA, 2011 Cranial neural crest cells on the move: their roles in craniofacial development. Am J Med Genet A 155A, 270–279. [PubMed: 21271641]

Crane JF, Trainor PA, 2006 Neural Crest Stem and Progenitor Cells. Annual Review of Cell and Developmental Biology 22, 267–286.

Dang I, Gorelik R, Sousa-Blin C, Derivery E, Guérin C, Linkner J, Nemethova M, Dumortier JG, Giger FA, Chipysheva TA, Ermilova VD, Vacher S, Campanacci V, Herrada I, Planson A-G, Fetics S, Henriot V, David V, Oguievetskaia K, Lakisic G, Pierre F, Steffen A, Boyreau A, Peyriéras N, Rottner K, Zinn-Justin S, Cherfils J, Bièche I, Alexandrova AY, David NB, Small JV, Faix J, Blanchoin L, Gautreau A, 2013 Inhibitory signalling to the Arp2/3 complex steers cell migration. Nature 503, 281–284. [PubMed: 24132237]

Author Manuscript Author Manuscript Author Manuscript Author Manuscript

Dyson L, Holmes A, Li A, Kulesa PM, 2018 A chemotactic model of trunk neural crest cell migration. Genesis 56, e23239. [PubMed: 30133140]

Epperlein H-H, Selleck MAJ, Meulemans D, McHedlishvili L, Cerny R, Sobkow L, Bronner-Fraser M, 2007 Migratory patterns and developmental potential of trunk neural crest cells in the axolotl embryo. Developmental Dynamics 236, 389–403. [PubMed: 17183528]

Forrester JV, Lois N, Zhao M, McCaig C, 2007 The spark of life: the role of electric fields in regulating cell behaviour using the eye as a model system. Ophthalmic Res 39, 4–16. [PubMed: 17164572]

Gilbert SF, Bender G, Betters E, Yin M, Cebra-Thomas JA, 2007 The contribution of neural crest cells to the nuchal bone and plastron of the turtle shell. Integrative and Comparative Biology 47, 401–408. [PubMed: 21672848]

Golding JP, Trainor P, Krumlauf R, Gassmann M, 2000 Defects in pathfinding by cranial neural crest cells in mice lacking the neuregulin receptor ErbB4. Nature Cell Biology 2, 103–109. [PubMed: 10655590]

Gov NS, 2007 Collective cell migration patterns: Follow the leader. Proceedings of the National Academy of Sciences 104, 15970.

Gruler H, Nuccitelli R, 1991 Neural crest cell galvanotaxis: new data and a novel approach to the analysis of both galvanotaxis and chemotaxis. Cell motility and the cytoskeleton 19, 121–133. [PubMed: 1878979]

Hall BK, 2000 The neural crest as a fourth germ layer and vertebrates as quadroblastic not triploblastic. Evolution & Development 2, 3–5. [PubMed: 11256415]

Hotary KB, Robinson KR, 1994 Endogenous Electrical Currents and Voltage Gradients in Xenopus Embryos and the Consequences of Their Disruption. Developmental Biology 166, 789–800. [PubMed: 7813796]

Hu N, Strobl-Mazzulla PH, Bronner ME, 2014 Epigenetic regulation in neural crest development. Dev Biol 396, 159–168. [PubMed: 25446277]

Ishii M, Arias AC, Liu L, Chen YB, Bronner ME, Maxson RE, 2012 A stable cranial neural crest cell line from mouse. Stem Cells Dev 21, 3069–3080. [PubMed: 22889333]

Jaffe LF, Stern CD, 1979 Strong electrical currents leave the primitive streak of chick embryos. Science 206, 569. [PubMed: 573921]

James AW, Shen J, Zhang X, Asatrian G, Goyal R, Kwak JH, Jiang L, Bengs B, Culiat CT, Turner AS, Seim Iii HB, Wu BM, Lyons K, Adams JS, Ting K, Soo C, 2015 NELL-1 in the treatment of osteoporotic bone loss. Nat Commun 6, 7362. [PubMed: 26082355]

Jiang X, Iseki S, Maxson RE, Sucov HM, Morriss-Kay GM, 2002 Tissue Origins and Interactions in the Mammalian Skull Vault. Developmental Biology 241, 106–116. [PubMed: 11784098]

Kasemeier-Kulesa JC, Bradley R, Pasquale EB, Lefcort F, Kulesa PM, 2006 Eph/ephrins and N-cadherin coordinate to control the pattern of sympathetic ganglia. Development 133, 4839–4847. [PubMed: 17108003]

Kasemeier-Kulesa JC, Kulesa PM, Lefcort F, 2005 Imaging neural crest cell dynamics during formation of dorsal root ganglia and sympathetic ganglia. Development 132, 235–245. [PubMed: 15590743]

Kennard AS, Theriot JA, 2020 Osmolarity-independent electrical cues guide rapid response to injury in zebrafish epidermis. bioRxiv, 2020.2008.2005.237792.

Krull CE, Collazo A, Fraser SE, Bronner-Fraser M, 1995 Segmental migration of trunk neural crest: time-lapse analysis reveals a role for PNA-binding molecules. Development 121, 3733–3743. [PubMed: 8582285]

Kulesa P, Ellies DL, Trainor PA, 2004 Comparative analysis of neural crest cell death, migration, and function during vertebrate embryogenesis. Developmental Dynamics 229, 14–29. [PubMed: 14699574]

Kulesa PM, Fraser SE, 1998 Neural Crest Cell Dynamics Revealed by Time-Lapse Video Microscopy of Whole Embryo Chick Explant Cultures. Developmental Biology 204, 327–344. [PubMed: 9882474]

Author Manuscript Author Manuscript Author Manuscript Author Manuscript

Kuo BR, Erickson CA, 2011 Vagal neural crest cell migratory behavior: a transition between the cranial and trunk crest. Developmental dynamics : an official publication of the American Association of Anatomists 240, 2084–2100. [PubMed: 22016183]

Le Douarin N, Kalcheim C, 1999 The neural crest, 2nd ed Cambridge University Press, Cambridge, UK ; New York, NY, USA.

Levin M, Pezzulo G, Finkelstein JM, 2017 Endogenous Bioelectric Signaling Networks: Exploiting Voltage Gradients for Control of Growth and Form. Annu Rev Biomed Eng 19, 353–387. [PubMed: 28633567]

Levin M, Selberg J, Rolandi M, 2019 Endogenous Bioelectrics in Development, Cancer, and Regeneration: Drugs and Bioelectronic Devices as Electroceuticals for Regenerative Medicine. iScience 22, 519–533. [PubMed: 31837520]

Litsiou A, Hanson S, Streit A, 2005 A balance of FGF, BMP and WNT signalling positions the future placode territory in the head. Development 132, 4051. [PubMed: 16093325]

Marcucio RS, Cordero DR, Hu D, Helms JA, 2005 Molecular interactions coordinating the development of the forebrain and face. Developmental Biology 284, 48–61. [PubMed: 15979605]

Mathews J, Levin M, 2018 The body electric 2.0: recent advances in developmental bioelectricity for regenerative and synthetic bioengineering. Current Opinion in Biotechnology 52, 134–144. [PubMed: 29684787]

McCaig CD, Robinson KR, 1982 The ontogeny of the transepidermal potential difference in frog embryos. Developmental Biology 90, 335–339. [PubMed: 7075864]

Mehta AS, Luz-Madrigal A, Li J-L, Tsonis PA, Singh A, 2019 Comparative transcriptomic analysis and structure prediction of novel Newt proteins. PloS one 14, e0220416–e0220416. [PubMed: 31419228]

Mehta AS, Singh A, 2017 Real time quantitative PCR to demonstrate gene expression in an undergraduate lab. Dros. Inf. Serv 100, 5.

Mehta AS, Singh A, 2019 Insights into regeneration tool box: An animal model approach. Developmental Biology 453, 111–129. [PubMed: 30986388]

Metcalf MEM, Borgens RB, 1994 Weak applied voltages interfere with amphibian morphogenesis and pattern. Journal of Experimental Zoology 268, 323–338.

Metcalf MEM, Shi R, Borgens RB, 1994 Endogenous ionic currents and voltages in amphibian embryos. Journal of Experimental Zoology 268, 307–322.

Minoux M, Rijli FM, 2010 Molecular mechanisms of cranial neural crest cell migration and patterning in craniofacial development. Development 137, 2605. [PubMed: 20663816]

Nichols DH, 1986 Formation and distribution of neural crest mesenchyme to the first pharyngeal arch region of the mouse embryo. American Journal of Anatomy 176, 221–231.

Noden DM, 1988 Interactions and fates of avian craniofacial mesenchyme. Development 103 Suppl, 121–140. [PubMed: 3074905]

Nuccitelli R, 1992 Endogenous ionic currents and DC electric fields in multicellular animal tissues. Bioelectromagnetics 13, 147–157. [PubMed: 1590813]

Nuccitelli R, 2003 Endogenous electric fields in embryos during development, regeneration and wound healing. Radiation Protection Dosimetry 106, 375–383. [PubMed: 14690282]

Nuccitelli R, Smart T, 1989 Extracellular Calcium Levels Strongly Influence Neural Crest Cell Galvanotaxis. The Biological Bulletin 176, 130–135. [PubMed: 29300581]

Nuccitelli R, Smart T, Ferguson J, 1993 Protein kinases are required for embryonic neural crest cell galvanotaxis. Cell Motility 24, 54–66.

Nuccitelli R, Wiley LM, 1985 Polarity of isolated blastomeres from mouse morulae: Detection of transcellular ion currents. Developmental Biology 109, 452–463. [PubMed: 2581832]

Pollard TD, Cooper JA, 2009 Actin, a Central Player in Cell Shape and Movement. Science 326, 1208. [PubMed: 19965462]

Regen CM, Steinhardt RA, 1986 Global properties of the Xenopus blastula are mediated by a high-resistance epithelial seal. Developmental Biology 113, 147–154.

Author Manuscript Author Manuscript Author Manuscript Author Manuscript

Reyes M, Zandberg K, Desmawati I, de Bellard ME, 2010 Emergence and migration of trunk neural crest cells in a snake, the California Kingsnake (Lampropeltis getula californiae). BMC Dev Biol 10, 52–52. [PubMed: 20482793]

Rothstein M, Bhattacharya D, Simoes-Costa M, 2018 The molecular basis of neural crest axial identity. Dev Biol 444 Suppl 1, S170–S180. [PubMed: 30071217]

Ruhrberg C, Schwarz Q, 2010 In the beginning: Generating neural crest cell diversity. Cell Adh Migr 4, 622–630. [PubMed: 20930541]

Sadaghiani B, Thiébaud CH, 1987 Neural crest development in the Xenopus laevis embryo, studied by interspecific transplantation and scanning electron microscopy. Developmental Biology 124, 91–110. [PubMed: 3666314]

Santagati F, Rijli FM, 2003 Cranial neural crest and the building of the vertebrate head. Nat Rev Neurosci 4, 806–818. [PubMed: 14523380]

Schilling TF, Kimmel CB, 1994 Segment and cell type lineage restrictions during pharyngeal arch development in the zebrafish embryo. Development 120, 483. [PubMed: 8162849]

Shellard A, Mayor R, 2019 Integrating chemical and mechanical signals in neural crest cell migration. Current opinion in genetics & development 57, 16–24. [PubMed: 31306988]

Shellard A, Szabo A, Trepat X, Mayor R, 2018 Supracellular contraction at the rear of neural crest cell groups drives collective chemotaxis. Science 362, 339–343. [PubMed: 30337409]

Shi R, Borgens RB, 1995 Three-dimensional gradients of voltage during development of the nervous system as invisible coordinates for the establishment of embryonic pattern. Developmental Dynamics 202, 101–114. [PubMed: 7734729]

Simões-Costa M, Bronner ME, 2015 Establishing neural crest identity: a gene regulatory recipe. Development (Cambridge, England) 142, 242–257.

Song B, Gu Y, Pu J, Reid B, Zhao Z, Zhao M, 2007 Application of direct current electric fields to cells and tissues in vitro and modulation of wound electric field in vivo. Nature Protocols 2, 1479–1489. [PubMed: 17545984]

Stundl J, Pospisilova A, Matejkova T, Psenicka M, Bronner ME, Cerny R, 2020 Migratory patterns and evolutionary plasticity of cranial neural crest cells in ray-finned fishes. Dev Biol.

Szabo A, Mayor R, 2018 Mechanisms of Neural Crest Migration. Annu Rev Genet 52, 43–63. [PubMed: 30476447]

Szabó A, Theveneau E, Turan M, Mayor R, 2019 Neural crest streaming as an emergent property of tissue interactions during morphogenesis. PLoS Comput Biol 15, e1007002–e1007002. [PubMed: 31009457]

Teddy JM, Kulesa PM, 2004 In vivo evidence for short- and long-range cell communication in cranial neural crest cells. Development 131, 6141–6151. [PubMed: 15548586]

Theveneau E, Marchant L, Kuriyama S, Gull M, Moepps B, Parsons M, Mayor R, 2010 Collective chemotaxis requires contact-dependent cell polarity. Developmental cell 19, 39–53. [PubMed: 20643349]

Tosney KW, 1982 The segregation and early migration of cranial neural crest cells in the avian embryo. Developmental Biology 89, 13–24. [PubMed: 7054004]

Trainor PA, 2005 Specification of neural crest cell formation and migration in mouse embryos. Semin Cell Dev Biol 16, 683–693. [PubMed: 16043371]

Trainor PA, 2010 Craniofacial birth defects: The role of neural crest cells in the etiology and pathogenesis of Treacher Collins syndrome and the potential for prevention. Am J Med Genet A 152A, 2984–2994. [PubMed: 20734335]

Trainor PA, Sobieszczuk D, Wilkinson D, Krumlauf R, 2002 Signalling between the hindbrain and paraxial tissues dictates neural crest migration pathways. Development 129, 433. [PubMed: 11807035]

Walheim CC, Zanin JP, de Bellard ME, 2012 Analysis of trunk neural crest cell migration using a modified Zigmond chamber assay. J Vis Exp, 3330. [PubMed: 22297254]

Walker MB, Trainor PA, 2006 Craniofacial malformations: intrinsic vs extrinsic neural crest cell defects in Treacher Collins and 22q11 deletion syndromes. Clinical Genetics 69, 471–479. [PubMed: 16712696]

Author Manuscript Author Manuscript Author Manuscript Author Manuscript

Wong GL, Cohn DV, 1975 Target cells in bone for parathormone and calcitonin are different: enrichment for each cell type by sequential digestion of mouse calvaria and selective adhesion to polymeric surfaces. Proc Natl Acad Sci U S A 72, 3167–3171. [PubMed: 171656]

Wynn ML, Rupp P, Trainor PA, Schnell S, Kulesa PM, 2013 Follow-the-leader cell migration requires biased cell-cell contact and local microenvironmental signals. Phys Biol 10, 035003–035003. [PubMed: 23735560]

Zhang X, Kuroda S, Carpenter D, Nishimura I, Soo C, Moats R, Iida K, Wisner E, Hu FY, Miao S, Beanes S, Dang C, Vastardis H, Longaker M, Tanizawa K, Kanayama N, Saito N, Ting K, 2002 Craniosynostosis in transgenic mice overexpressing Nell-1. J Clin Invest 110, 861–870. [PubMed: 12235118]

Zhao S, Mehta AS, Zhao M, 2020 Biomedical applications of electrical stimulation. Cellular and Molecular Life Sciences.

Author Manuscript Author Manuscript Author Manuscript Author Manuscript

Highlights

1. Direct current (DC) electric fields guide migration of mammalian cranial neural crest cells (CNCC).
2. CNCC are directed towards the anode at and above threshold voltage of 30mV/mm.
3. Directedness, and displacement speed of CNCC increase with the increase in electric field strength.

Author Manuscript Author Manuscript Author Manuscript Author Manuscript

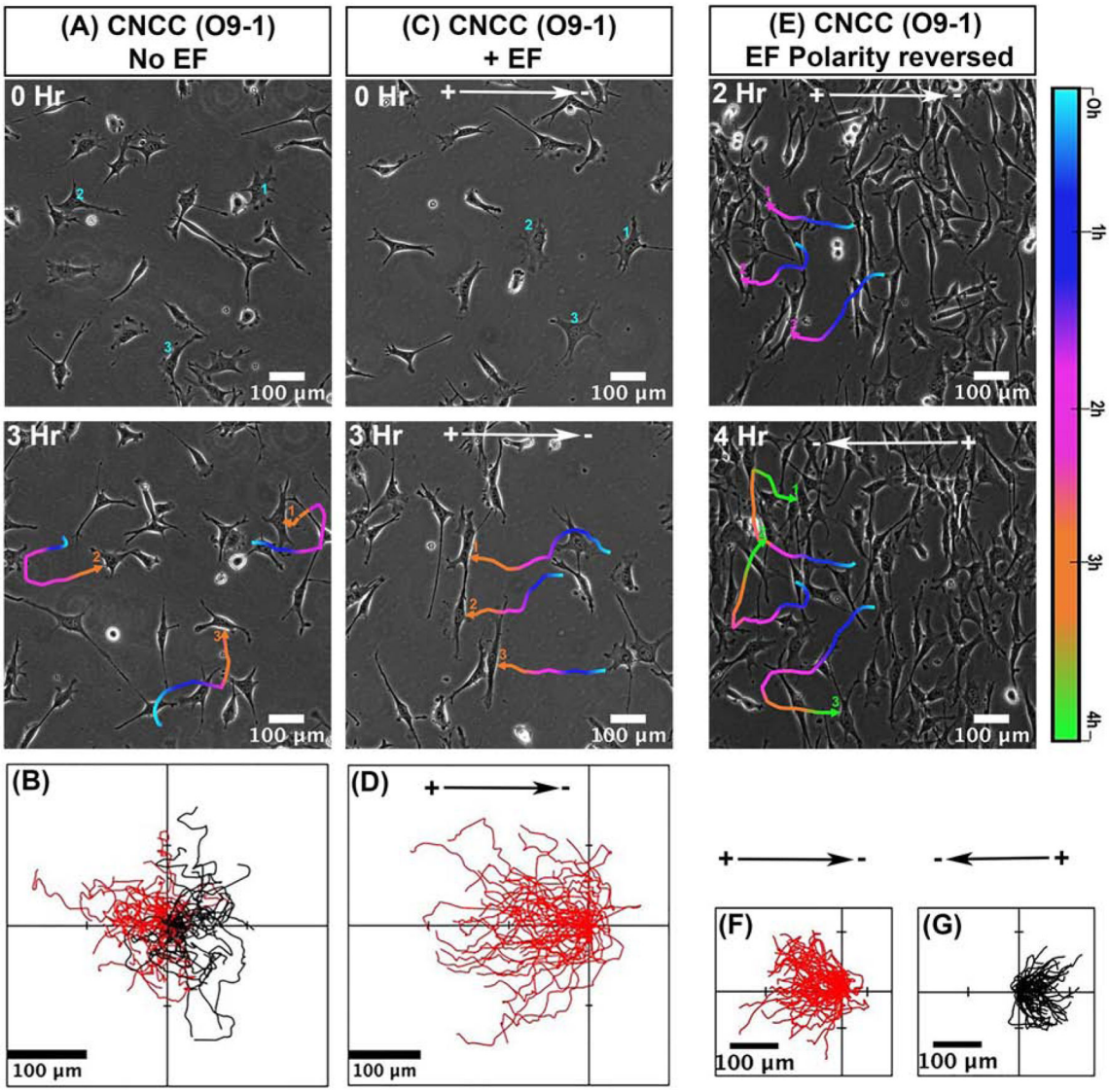

Fig 1. Galvanotaxis of mammalian cranial neural crest cell (CNCC) line - 'O9–1'.

(A,B) Migration of CNCCs in control cultures without applying EF **(C,D)** Significant directional migration of CNCC to the anode in an applied EF. B and D show the migration tracks of CNCCs for 3 hours as in A and C respectively. **(E,F,G)** Reversal of EF polarity reversed cell migration direction. **(F)** In the first 2 hours cells move toward the anode on the left. Then the field polarity was reversed for next 2 hours. **(G)** Cells reversed their direction within 5–10 minutes following reversal of field polarity and migrated towards the new anode on the right. Migration trajectories of selected cells in A, C and E are presented as temporal color codes. F and G show migration tracks as from E for total of 4 hrs with field polarity reversed after 2 hrs. Cells migrate towards the left are shown in red, and to the right in black. The position of all cells in B,D, F, G, at t = 0 min is positioned at the origin (0, 0). n= 50 cells from one experiment and confirmed in two additional experiments. O9–1 cells were cultured in complete ES cell medium with 15% FBS and LIF + 25 ng/ml recombinant human bFGF. EF= 200 mV/mm.

Author Manuscript Author Manuscript Author Manuscript Author Manuscript

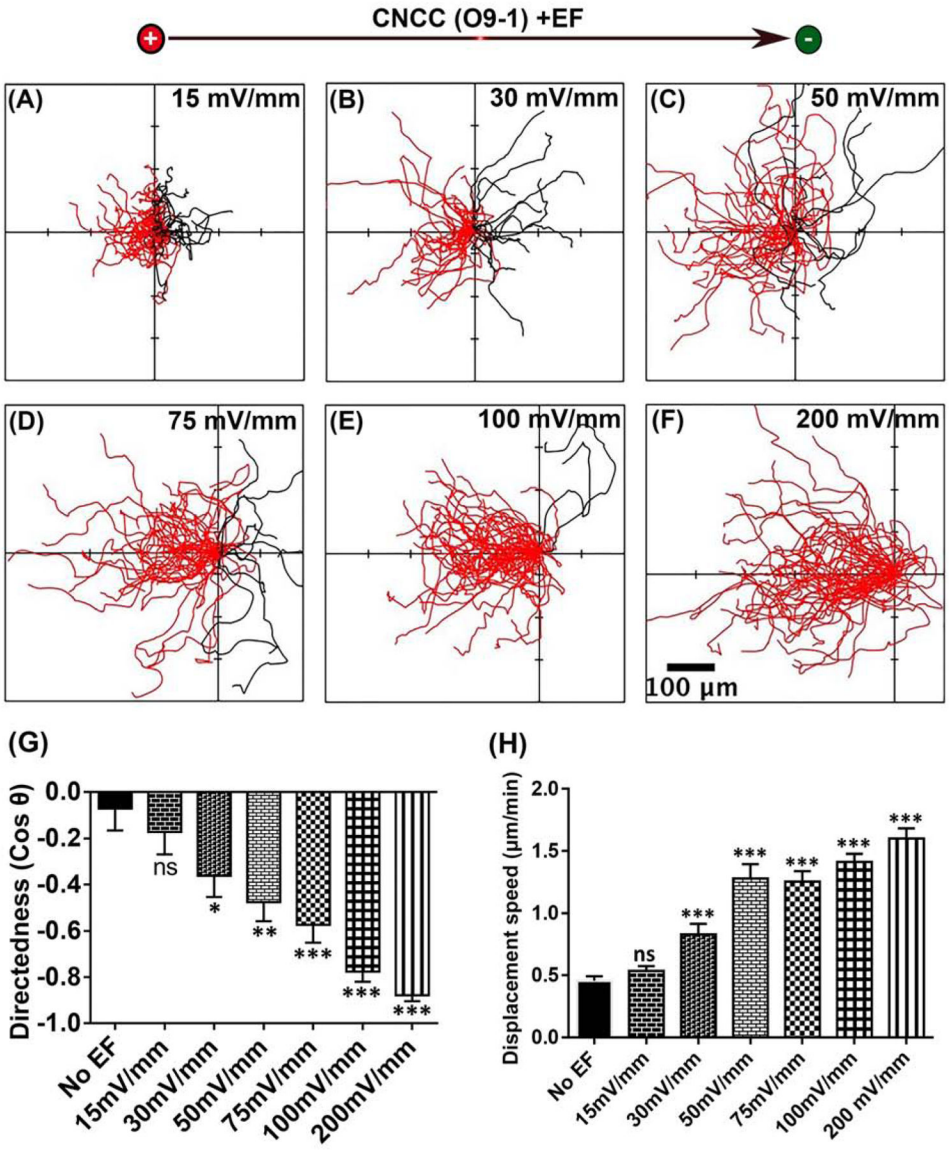

Fig 2. Voltage dependence of galvanotaxis of mammalian CNCC (O9–1 cell line).

(A–F). Migration trajectories of CNCCs for 3 hrs. All cells started from the origin. Cells migration towards the anode to the left are shown in red, and towards the cathode to the right in black **(G).** The migration directedness, and **(H)** displacement speed of CNCCs increase with the increasing field strength. Data are mean ± SEM. *P<0.05, **P<0.01, ***P<0.001.

Author Manuscript Author Manuscript Author Manuscript Author Manuscript

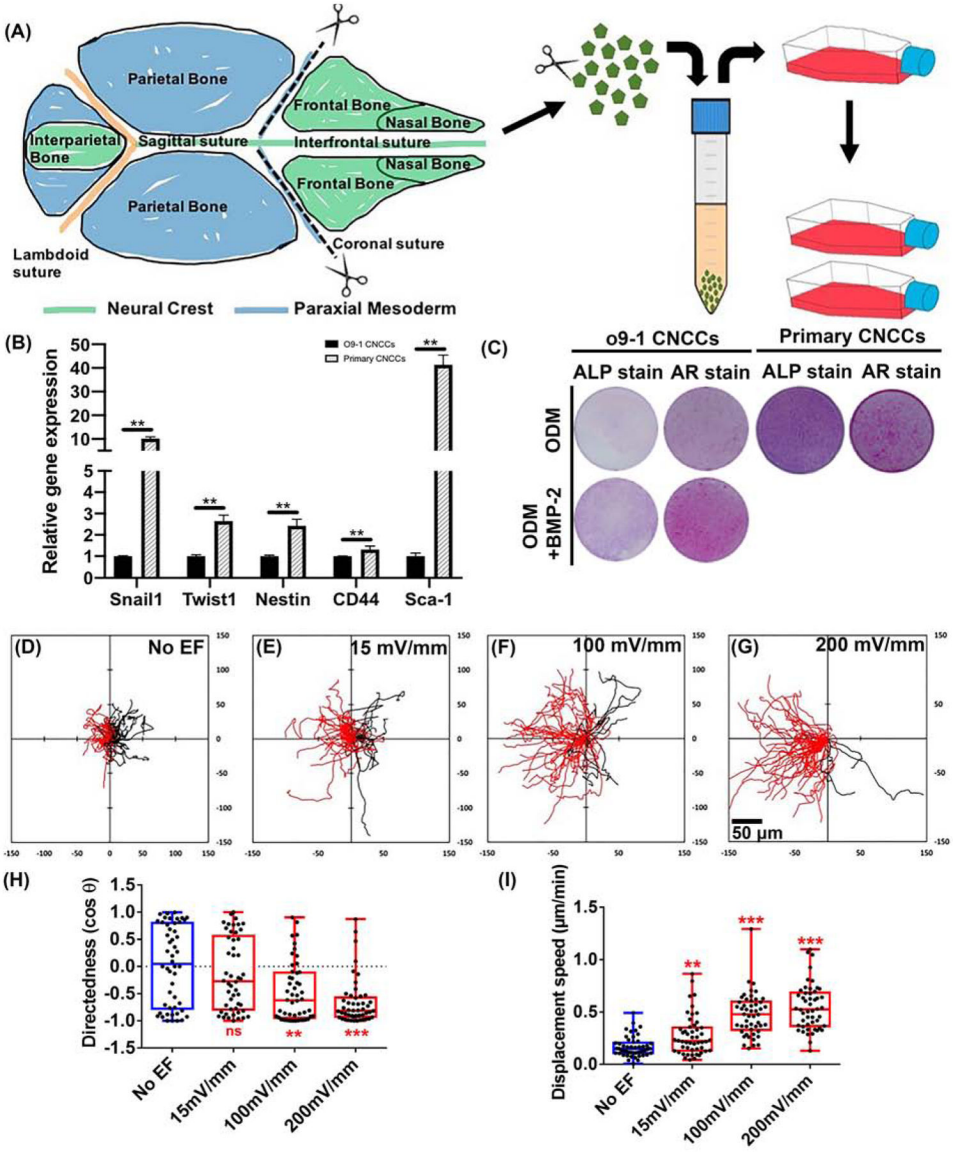

Fig 3. Galvanotaxis of primary CNCCs.

(A) Primary CNCCs were isolated from the frontal and nasal bones of neonatal mouse cranial vault (green part labeled). They were expanded in growth medium (passages 3–5). Cranial lineage of primary culture of CNCCs were validated by **(B)** RT-qPCR and **(C)** Osteogenic differentiation. **(B)** Gene expression of NCC markers (*Snail1, Twist1, Nestin, CD44* and *Sca-1)* in primary NCCs was normalized to O9–1 CNCCs. N=3, each template underwent reverse transcription from an RNA pool of 3 experimental sets of cells. **(C)** Osteogenic differentiation of O9–1 and primary CNCCs were initiated by culturing the cells in osteogenic differentiation medium (ODM) (+/− 100ng/ml BMP2). ALP staining was performed on Day-7, and AR staining was performed on Day-21. Images are representative from triplicates of each group. **(D–G)** Migration trajectories. Cells migrate towards the anode to the left as shown in red, and towards cathode to the right in black. All cells started from the origin and migrated for 3 hours. **(H)** Applied EFs directed cell migration **(I)**

increased displacement speed. *P<0.05, **P<0.01, *** P<0.001 when compared to the no EF control. Scale bar 50 μm.

Author Manuscript Author Manuscript Author Manuscript Author Manuscript

Author Manuscript Author Manuscript Author Manuscript Author Manuscript

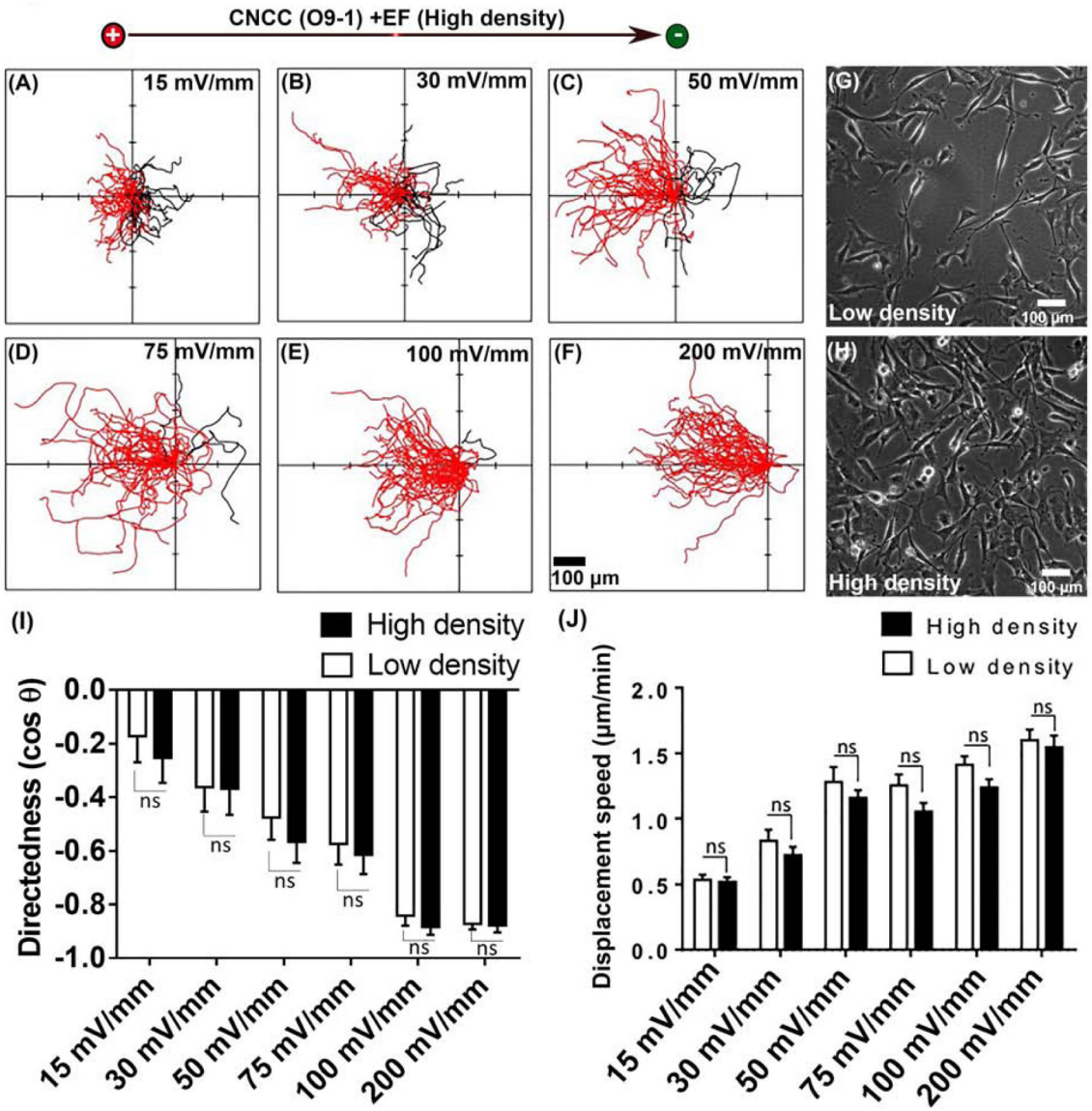

Fig 4. CNCCs in high density cultures showed similar galvanotaxis.

(A–F) Cell migration trajectories in high density culture, with starting position from the origin for 3 hours. All cells started from the origin. Cells migration towards the anode to the left are shown in red, and towards the cathode to the right in black. 50 CNCCs from one experiment, repeated with two more experiments. Representative example of **(G)** low density CNCCs and **(H)** high density CNCCs. **(I)** Migration directedness, and **(J)** displacement speed of cells in high density cultures are very similar to that of cells in low density culture in fields of all strengths tested.

Author Manuscript

Author Manuscript

Author Manuscript

Author Manuscript

Table 1.

List of RT-qPCR primers.

Primer	Sequence (Forward)	Sequence (Reverse)
GAPDH	5’-ATTCAACGGCACAGTCAAGG-3’	5’-GATGTTAGTGGGGTCTCGCTC-3’
Snail1	5’-CTTGTGTCTGCACGACCTGT-3’	5’-CTTCACATCCGAGTGGGTTT-3’
Twist1	5’-GGAGGATGGAGGGGGCCTGG-3’	5’-TGTGCCCCACGCCCTGATTC-3’
Nestin	5’-AATGGGAGGATGGAGAATGGAC-3’	5’-TAGACAGGCAGGGCTAGCAAG-3’
CD44	5’-GTGGCACACAGCTTGGGGA-3’	5’-TCAGAGCCAGTGCCAGGAGAGAT-3’
Sca-1	5’-CTCTGAGGATGGACACTTCT-3’	5’-GGTCTGCAGGAGGACTGAGC-3’